Article

Electron Emission Originated from Free-Electron-like States of Alkali-Doped Boron#Nitride Nanotubes

Binghai Yan, Changwon Park, Jisoon Ihm, Gang Zhou, Wenhui Duan, and Noejung Park

J. Am. Chem. Soc., **2008**, 130 (50), 17012-17015 • DOI: 10.1021/ja805557g • Publication Date (Web): 14 November 2008

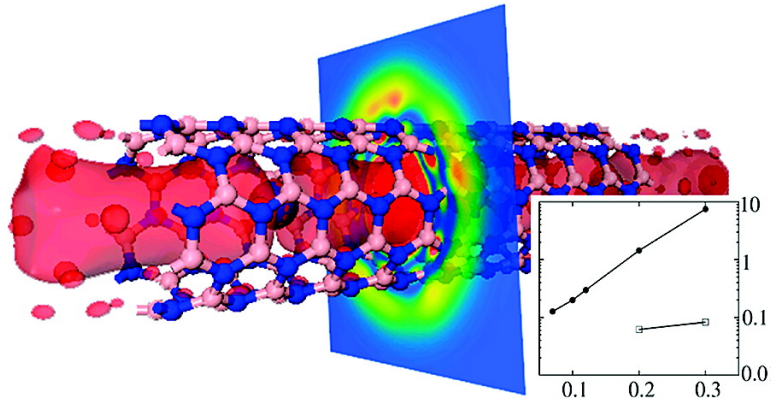

More About This Article

Additional resources and features associated with this article are available within the HTML version:

- Supporting Information
- Access to high resolution figures
- Links to articles and content related to this article
- Copyright permission to reproduce figures and/or text from this article

View the Full Text HTML

J|A|C|S
ARTICLES

Published on Web 11/14/2008

Electron Emission Originated from Free-Electron-like States of Alkali-Doped Boron−Nitride Nanotubes

Binghai Yan,[†,‡] Changwon Park,[†] Jisoon Ihm,[†] Gang Zhou,[§] Wenhui Duan,[§] and Noejung Park*[,⊥]

Department of Physics and Astronomy, Seoul National University, Seoul 151-742, Korea, Center for Advanced Study, Tsinghua University, Beijing 100084, People's Republic of China, and Department of Physics, Tsinghua University, Beijing 100084, People's Republic of China, and Department of Applied Physics, Dankook University, 126, Jukjeon-dong, Yongin-si, Gyeonggi-do, 448-701, Korea

Received July 17, 2008; E-mail: noejung@dku.edu

Abstract: We investigate the electronic structures and electron emission properties of alkali-doped boron−nitride nanotubes (BNNTs) using density-functional theory calculations. We find that the nearly free-electron (NFE) state of the BNNT couples with the alkali atom states, giving rise to metallic states near the Fermi level. Unlike the cases of potassium-doped carbon nanotubes, not only the s but the d orbital state substantially takes part in the hybridization, and the resulting metallic states preserve the free-electron-like energy dispersion. Through first-principles electron dynamic simulations under applied fields, it is shown that the alkali-doped BNNT can generate an emission current 2 orders of magnitude larger than the carbon nanotube. The nodeless wave function at the Fermi level, together with the lowered work function, constitutes the major advantage of the alkali-doped BNNT in electron emission. We propose that the alkali-doped BNNT should be an excellent electron emitter in terms of the large emission current as well as its chemical and mechanical stability.

1. Introduction

Recent successes in the production of the boron−nitride nanotube (BNNT), which is a geometrical clone of the more widely known carbon nanotube (CNT), have attracted a lot of attention because of its unique properties as a one-dimensional wide band gap nanostructure.[1] Although high mechanical and chemical stability are undoubtedly great merits of the BNNT,[2] a more interesting fact is that its electronic structure has an unusual feature not shared by most wide band gap materials. Theoretical calculations have repeatedly predicted that the nearly free-electron (NFE) state should exist near the edge of the conduction band of the BNNT.[3] Owing to the free-electron-like energy dispersion and uniformly delocalized wave function character across the interior space of the BNNT, it could serve as an ideal electron transport channel that may potentially be utilized for various electronic device applications.

In the present work, we particularly focus on the field emission properties of the BNNT in relation to its unique electronic structure. The geometrical advantage of such a narrow nanostructure in electron field emission has been widely noticed in experiments with CNTs.[4] Nevertheless, the lack of long-time stability under affordable vacuum conditions has been a great challenge to people who seek CNT-based field emission devices.[5] The known robustness of boron−nitride materials against heating or oxidation, together with the free-electron-like conduction band states, leads us to consider the BNNT as a possible alternative for an electron field emitter. On the other hand, the band gap of the BNNT is too wide and thus we need to develop a transport channel near the Fermi level. Motivated by a few recent successes in the fabrication of the Cs-encapsulated CNTs,[6] we explore the electronic structure of various BNNTs with cesium (Cs) and potassium (K) dopants adsorbed inside the tube and investigate whether free-electron-like states could exist near the Fermi level. In later parts, we study the electron emission properties of the BNNTs, calculating the emission current under applied electric fields. We present an explicit comparison with the CNT and show that the BNNT gives 2 orders of magnitude larger emission current. We discuss that the alkali-doped BNNT has two distinguishable advantages in electron emission: one is the lowered work function and the other is the nodeless wave function of the down-shifted NFE state.

[†] Seoul National University.
[‡] Center for Advanced Study, Tsinghua University.
[§] Department of Physics, Tsinghua University.
[⊥] Dankook University.

(1) (a) Golberg, D.; Bando, Y.; Tang, C.; Zhi, C. *Adv. Mater.* **2007**, *19*, 2413. (b) Arenal, R.; Ferrari, A. C.; Reich, S.; Wirtz, L.; Mevellec, J.-Y.; Lefrant, S.; Rubio, A.; Loiseau, A. *Nano Lett.* **2006**, *6*, 1812. (c) Cumings, J.; Zettl, A. *Solid State Commun.* **2004**, *129*, 661. (d) Wirtz, L.; Marini, A.; Rubio, A. *Phys. Rev. Lett.* **2006**, *96*, 126104. (e) Park, C.-H.; Spataru, C. D.; Louie, S. G. *Phys. Rev. Lett.* **2006**, *96*, 126105.
(2) (a) Golberg, D.; Bando, Y.; Kurashima, K.; Sato, T. *Scripta Mater.* **2001**, *44*, 1561. (b) Chen, Y.; Zou, J.; Campbel, S. J.; Caer, G. L. *Appl. Phys. Lett.* **2004**, *84*, 2430. (c) Miyoshi, K.; Buckley, D. H.; Pouch, J. J.; Alterovitz, S. A.; Sliney, H. E. *Surf. Coat. Technol.* **1990**, *33*, 221.
(3) (a) Rubio, A.; Corkill, J. L.; Cohen, M. L. *Phys. Rev. B* **1994**, *49*, 5081. (b) Blase, X.; Rubio, A.; Louie, S. G.; Cohen, M. L. *Europhys. Lett.* **1994**, *28*, 335.

10.1021/ja805557g CCC: $40.75

2. Computational Methods

Our calculations are based on the total energy calculation within the density functional theory (DFT).[7] We use the ultrasoft pseudopotentials and local density approximation (LDA).[8] Both the Vienna Ab Initio Simulation Package (VASP)[9] and PWscf package[10] are used and cross-checked. The plane-wave basis set is employed with the energy cutoff of 400 eV.[11] For field emission calculations, we use the local orbital basis set[12] to save the computational load and then convert it to the plane-wave one, allowing the time evolution of electronic states into the vacuum region according to the evolution operator $\exp(-i\hat{H}t/\hbar)$.[13] Here $\hat{H}$ is the self-consistent Hamiltonian including the external field.

3. Results

We first consider the effect of the Cs-encapsulation inside BNNTs. Parts a,b, c,d, and e,f of Figure 1 show the pairs of the electronic band structures of the pure and the Cs-encapsulated (5,5), (9,0), and (12,0) BNNTs, respectively. The chosen computational unit cell length along the axial direction for the (5,5) BNNT is 4 times the primitive unit cell of the arm-chair nanotube (9.93 Å), whereas that used for the (9,0) or (12,0) BNNT is twice the primitive unit cell of the zigzag nanotubes (8.60 Å). We put one Cs atom in the computational unit cell, as shown by large purple spheres in the insets of Figure 1b,d,f. In order to simulate isolated BNNTs, we use a large supercell along the perpendicular direction to the tube axis, in which the interwall distance between the periodic images of the BNNT is larger than 15 Å. Through the geometry optimization, the Cs atom sits at the tube center for the (5,5) and (9,0) BNNTs, while at the point of 3.5 Å away from the interior wall for the case of the (12,0) BNNT.

The encapsulation of the Cs atom gives rise to a metallic band crossing the Fermi level. For the case of the pure (5,5) BNNT, the NFE state is at the conduction band minimum (CBM), as indicated by the downward arrow in Figure 1a. Upon the Cs encapsulation, the NFE state shifts down to form a hybridized state with the Cs atomic orbitals, as indicated in Figure 1b. A simple comparison between parts a and b of Figure 1 shows that the NFE state shifts down almost rigidly upon the Cs doping, while the other bands remain intact or change only modestly. Note that the dispersions of the pure NFE and the down-shifted hybridized one are almost identical near the zone center ($0.0 \leq k \leq 0.3$). This indicates that the hybridized NFE state in Figure 1b is derived mainly from the NFE state of the (5,5) BNNT, and the contribution of the Cs atomic orbital is not very significant. For the case of the (9,0) BNNT, the CBM state (indicated by the leftward arrow in Figure 1c) is predominated by the boron p_z orbitals. The NFE state is about 0.7 eV above the CBM, as noted by the downward arrow. The CBM state, hybridized with the Cs atoms' 6s and 5d orbitals, shifts down and develops the metallic band, as indicated by the leftward arrow in Figure 1d. The NFE state is also hybridized with the Cs atomic orbitals (6s and $5d_{z^2}$), constituting the low-lying conduction band, as noted by the downward arrow in Figure 1d. Besides these two bands (NFE and CBM), other bands remain almost intact. In the case of the (12,0) BNNT, the pure NFE state is 0.4 eV above the CBM, as indicated by the downward arrow in Figure 1e. Upon the Cs doping, one metallic band is developed at the Fermi level, as denoted by the downward arrow in Figure 1f. Unlike the case of the (9,0) BNNT, the NFE state is solely hybridized with the Cs atomic orbitals to form the metallic band. Consistent with the case of the (5,5) BNNT, the dispersions of the pure NFE and the down-

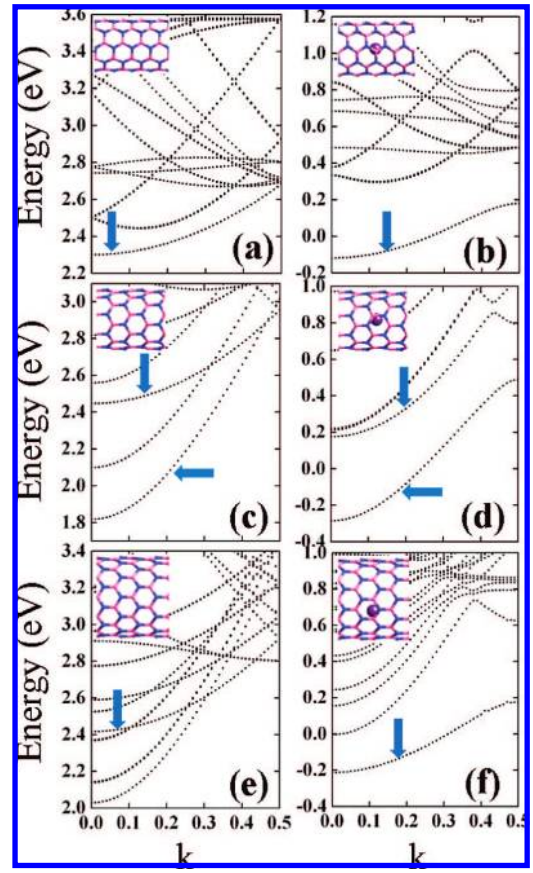

Figure 1. The electronic band structure of (a) the pure and (b) the Cs-encapsulated (5,5) BNNT, (c) the pure and (d) the Cs-encapsulated (9,0) BNNT, and (e) the pure and (f) the Cs-encapsulated (12,0) BNNT, respectively. Insets show unit-cell geometries chosen in this calculation. The Fermi level is set to zero. The Fermi level in panels a, c, or e is fixed to the center of the density-functional energy gap, while that in panels b, d, or f is determined in the self-consistent calculation with eight *k*-points along the axial direction.

(4) (a) Wang, Q. H.; Corrigan, T. D.; Dai, J. Y.; Chang, R. P. H.; Krauss, A. R. *Appl. Phys. Lett.* **1997**, *70*, 3308. (b) Zhu, W.; Bower, C.; Zhou, O.; Kochanski, G.; Jin, S. *Appl. Phys. Lett.* **1999**, *75*, 873. (c) Bonard, J.-M.; Maier, F.; Stöckli, T.; Châtelain, A.; de Heer, W. A.; Salvetat, J.-P.; Forró, L. *Ultramicroscopy* **1998**, *73*, 7. (d) Yoon, B.-J.; Hong, E. H.; Jee, S. E.; Yoon, D.-M.; Shim, D.-S.; Son, G.-Y.; Lee, Y. J.; Lee, K.-H.; Kim, H. S.; Park, C. G. *J. Am. Chem. Soc.* **2005**, *127*, 8234.
(5) (a) Dean, K. A.; Chalamala, B. R. *Appl. Phys. Lett.* **1999**, *75*, 3017. (b) Dean, K. A.; Chalamala, B. R. *Appl. Phys. Lett.* **2000**, *76*, 375. (c) Yi, W. K.; Jeong, T. W.; Yu, S. G.; Heo, J. N.; Lee, C. S.; Lee, J. H.; Kim, W. S.; Yoo, J.-B.; Kim, J. M. *Adv. Mater.* **2002**, *14*, 1464. (d) Purcell, S. T.; Vincent, P.; Journet, C.; Binh, V. T. *Phys. Rev. Lett.* **2002**, *88*, 105502.
(6) (a) Jeong, G.-H.; Farajian, A. A.; Hatakeyama, R.; Hirata, T.; Yaguchi, T.; Tohji, K.; Mizuseki, H.; Kawazoe, Y. *Phys. Rev. B* **2003**, *68*, 075410. (b) Jeong, G.-H.; Hatakeyama, R.; Hirata, T.; Tohji, K.; Motomiya, K.; Yaguchi, T.; Kawazoe, Y. *Chem. Commun. (Cambridge)* **2003**, 152. (c) Izumida, T.; Hatakeyama, R.; Neo, Y.; Mimura, H.; Omote, K.; Kasama, Y. *Appl. Phys. Lett.* **2006**, *89*, 093121.
(7) Kohn, W.; Sham, L. J. *Phys. Rev.* **1965**, *140*, 1133.
(8) Ceperley, D. M.; Alder, B. J. *Phys. Rev. Lett.* **1980**, *45*, 566.
(9) (a) Kresse, G.; Furthmüller, J. *Phys. Rev. B* **1996**, *54*, 11169. (b) Kresse, G.; Furthmüller, J. *Comput. Mater. Sci.* **1996**, *6*, 15.
(10) Baroni, S.; de Gironcoli, S.; Dal Corso, A.; Giannozzi, P. http://www.pwscf.org.
(11) Ihm, J.; Zunger, A.; Cohen, M. L. *J. Phys. C. Solid State Phys.* **1979**, *12*, 4409.
(12) Soler, J. M.; Artacho, E.; Gale, J. D.; Garcia, A.; Junquera, J.; Ordejón, P.; Sánchez-Portal, D. *J. Phys.: Condens. Matter* **2002**, *14*, 2745.
(13) (a) Han, S.; Lee, M. H.; Ihm, J. *Phys. Rev. B* **2002**, *65*, 085405. (b) Lee, S. B.; Kim, S.; Ihm, J. *Phys. Rev. B* **2007**, *75*, 075408.

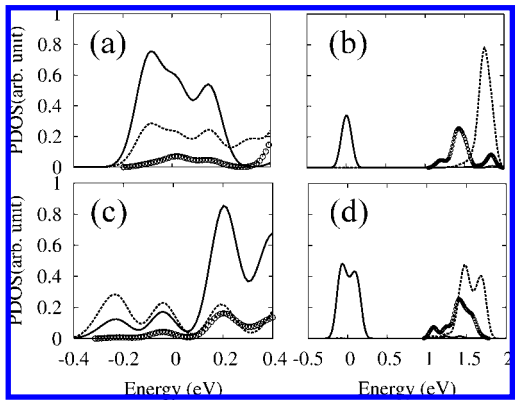

Figure 2. The PDOS of Cs 6s orbital (solid line), 6p orbitals (open circles), and 5d orbitals (dashed line) for (a) the Cs-encapsulated (5,5) BNNT and (b) the isolated Cs atom in the same computational unit cell. The same PDOS for (c) the Cs-encapsulated (9,0) BNNT and (d) the isolated Cs atom. The Fermi level is set to be 0 eV.

shifted one are almost identical near the zone center. We note that the case of the (9,0) BNNT is rather peculiar. The energy level of the NFE state of the small zigzag type BNNT is particularly high; thus, the donated electrons from the alkali dopants mainly occupy the CBM state. In cases of larger zigzag BNNTs, for example (24,0) BNNT, we obtained similar results to the (12,0) BNNT (not shown).

In order to have a clearer understanding of the down-shifted NFE state, we calculated the projected density of states (PDOS) into the Cs atom's 6s, 6p, and 5d orbitals. Such PDOS for the case of the Cs-encapsulated (5,5) BNNT is shown in Figure 2a. For comparison, we calculated the PDOS for the isolated Cs atom in the same computational unit cell, as presented in Figure 2b. The same set of the PDOS for the case of the (9,0) BNNT are shown in Figure 2c,d. It is noteworthy that the 5d orbital states, along with the 6s ones, are dominantly involved in the hybridization with the NFE state, as shown in Figure 2a,c. Note that the down-shifted NFE state is at around and 0.2 eV above the Fermi level in each case of Figure 1b,d, respectively. Through a close examination of the Kohn−Sham wave function, we found that the d orbital contribution in Figure 2a,c is mostly from the $5d_{z^2}$. Here we define the axial direction of the nanotube as the z axis. This is consistent with the fact that only 6s and $5d_{z^2}$ orbitals, which are nodeless not only along the circumferential but the axial direction, have the same symmetry as the NFE state. Since we used the periodic boundary conditions, the isolated Cs atom in the computational unit cell can be regarded as a one-dimensional Cs chain with the interatomic distance of 9.93 Å (Figure 2b) and 8.60 Å (Figure 2d), respectively. The dispersions of the Cs chain states are rather small, as shown in Figure 2b,d, and the 6s and 5d orbital states are clearly separated by about 1.5 eV. In this regard, the aforementioned metallic bands of the Cs-encapsulated BNNTs are characteristically different from those of Cs chain states.

Recently, Margine et al. suggested that the down-shift of the NFE state of the CNT, upon potassium encapsulation, should mainly be attributed to the universal electrostatic behavior rather than the coupling with the s orbital of the dopant.[14] Their theory applies to our cases as well. The presence of the Cs atom, which is a strong electron donor, provides a positive potential in the inner space of the BNNTs. This positive potential at the tube center mainly affects the NFE state. We performed similar studies of the (5,5) and (9,0) BNNT with various dopant density (i.e., from $XB_{18}N_{18}$ to $XB_{80}N_{80}$, where X represents Cs or K) and found that an appropriate minimum density of positive potential centers is required to shift down the NFE state. Cs atom is found to be more effective than K, owing to the higher tendency of ionization. In the cases with the highest density of dopants ($XB_{18}N_{18}$ and $XB_{20}N_{20}$), the metallic bands at the Fermi level largely resemble those of the one-dimensional chain of bare Cs or K atoms. This is consistent with the previous studies of the densely packed K chain inside the CNT.[15] In contrast, the present results imply that the Cs dopants need not be so densely packed to derive the NFE-like Fermi level state in BNNTs.

Numerous previous works have intercalated alkali atoms inside or in the interstitial space of bundled CNTs.[6,16] By taking analogy to such experiments, the method of Cs-plasma ion irradiation[6] or deposition of vaporized Cs atoms[16] could be a right choice of experiment to synthesize the Cs-encapsulated BNNTs. In this regard, it is pertinent to investigate the stability of the encapsulated Cs atom with respect to the isolated one. Our LDA results for the adsorption energy of the Cs atom onto the inner and outer wall of the (12,0) BNNT are 0.52 and 0.26 eV, respectively.[17] This indicates that Cs atoms tend to encapsulate in the inner core of the BNNTs if the tubes are appropriately opened. Note that that our aforementioned theories are not limited to the single-walled BNNTs with encapsulated Cs atoms at the inner core. In the Supporting Information we provide our results for the cases of bundled double-walled BNNTs. It is shown that the NFE state shifts down either with Cs adatoms into the inner core or in the interstitial space of the bundles (Figures S4 and S5, Supporting Information).

We now investigate the field emission characteristics of the Cs-encapsulated BNNT. For this simulation, we choose the hydrogen-passivated (5,5) BNNT of 38.20 Å long, with Cs dopants encapsulated with nearly the same density as in Figure 1b. Figure 3a shows the computational supercell in the present case. Since we apply the external electric field along the axial direction and calculate the time evolution of each Kohn−Sham state, we need a large vacuum region. Figure 3b shows the total local potential, averaged in the xy plane and plotted along the axial direction (z) under the applied field $E = 0.10$ V/Å. The total charge inside the tube region (Q_{in}) is calculated at each time step. The time evolution of one of the NFE-derived states is presented in Figure 3c. The time variation of the tube region charge ($-dQ_{in}/dt$), weighted with the occupation factor of the band, is identified as the emission current. The total current summed over the bands is presented in Figure 3d. For comparison, we calculate the emission current of the (5,5) CNT with the same length as well. While the π-derived states dominantly contribute to the emission current of the (5,5) CNT, most of the emission current of the Cs-doped BNNT originated from the NFE-derived states. It is noteworthy that the Cs-encapsulated BNNT gives 2 orders of magnitude larger current than the CNT.

(14) Margine, E. R.; Crespi, V. H. *Phys. Rev. Lett.* **2006**, *96*, 196803.

(15) (a) Miyamoto, Y.; Rubio, A.; Blase, X.; Cohen, M. L.; Louie, S. G. *Phys. Rev. Lett.* **1995**, *74*, 2993. (b) Rubio, A.; Miyamoto, Y.; Blase, X.; Cohen, M. L.; Louie, S. G. *Phys. Rev. B* **1996**, *53*, 4023. (c) Miyake, T.; Saito, S. *Phys. Rev. B* **2002**, *65*, 165419.

(16) (a) Suzuki, S.; Watanabe, Y.; Ogino, T.; Heun, S.; Gregoratti, L.; Barinov, A.; Kaulich, B.; Kiskinova, M.; Zhu, W.; Bower, C.; Zhou, O. *J. Appl. Phys.* **2002**, *92*, 7527. (b) Duclaux, L. *Carbon* **2002**, *40*, 1751. (c) Monthioux, M. *Carbon* **2002**, *40*, 1809.

(17) We also calculated the adsorption energetics with the gradient-corrected density functional theory. Detailed results are presented in Figure S3, Supporting Information.

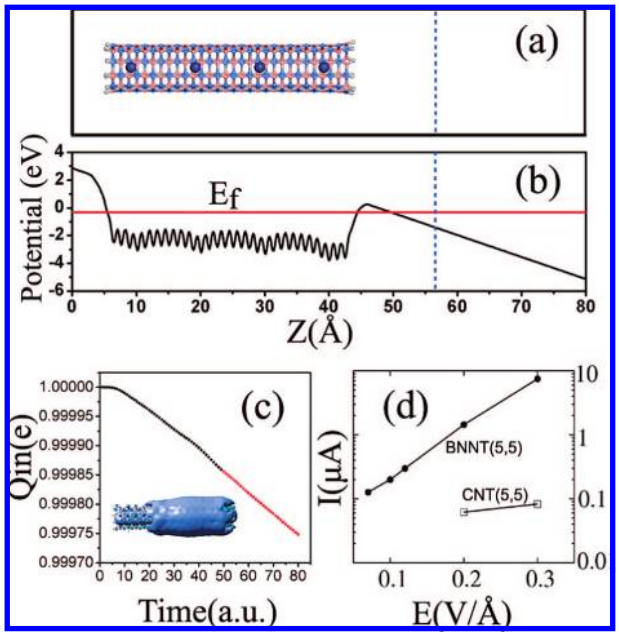

Figure 3. (a) The geometry of the finite-length hydrogen-passivated (5,5) BNNT with four Cs dopants within the supercell for the field emission calculation. (b) The total potential under the external field of $E = 0.10$ V/Å, averaged in the *xy* plane and plotted along the axial direction (z) of the BNNT. The solid horizontal line in part b indicates the Fermi level, and the vertical dashed line in parts a and b divides the tube region and vacuum region. (c) The time evolution of the tube region charge (Q_{in}) of one NFE-derived state. The isovalue surface of the charge density, at the beginning of the time evolution, is shown in the inset. Here the time step (1 au) is 0.0242 fs. The time-derivative of the tube region charge ($-dQ_{in}/dt$) is calculated from the linear region between 50 and 80 steps. (d) Total emission current for the Cs-encapsulated (5,5) BNNT and CNT under various external fields.

The superiority of the doped BNNT over the CNT for electron emission could be attributed to the lower vacuum barrier. We explicitly calculated the work function of both the CNT and the Cs-encapsulated BNNT. With the same geometry as used in the aforementioned field emission calculation, the work function of the finite length (5,5) CNT and the Cs-encapsulated BNNT are found to be 3.80 and 1.58 eV, respectively. We also calculated the work function of the perfect infinite length nanotubes. The LDA results for the work function of the perfect (5,5) CNT and Cs-encapsulated (5,5) BNNT are 4.61 and 2.24 eV, respectively, which is consistent with the previous work.[18] Note that the hydrogen passivation in the finite length nanotubes induced a substantial reduction of the work function. The Cs-encapsulated BNNT has a smaller work function than that of the (5,5) CNT by about 2.2 eV. In practice, the detailed height and thickness of the vacuum barrier depend on the local field at the tip. Nevertheless, the difference in the overall barrier height between the (5,5) CNT and Cs-encapsulated BNNT should be attributed to the aforementioned intrinsic difference in the work function. Besides the smaller work function, the Cs-encapsulated BNNT has an additional advantage in electron emission. The time evolution of the s-like state, which is nodeless along the circumferential direction of the nanotube, indicates that its contribution to the current is greater than those of higher angular momentum states because of its easier coupling with the vacuum state.[13] The electronic states at the Fermi level of the Cs-encapsulated (5,5) BNNT are derived from the NFE band, and thus all are s-like ones. A recent experiment demonstrated an outstanding electron emission from a few layers of stacked BN ribbons on the surface of porous BN spheres.[19] The down-shifted NFE state may also have contributed to the electron emission from such configurations. We performed computations with stacked BN ribbons and found that the NFE state of the ribbon shifts down under an applied electric field. It is probable that the s-like wave packet at the field emitting edges of the BN ribbons could evolve well into the free-electron state of the vacuum (Figures S6 and S7, Supporting Information).

4. Conclusion

In summary, we investigated how to utilize the NFE state of the BNNT, considering the Cs- or K-encapsulated (5,5), (9,0), and (12,0) BNNTs. It was shown that the NFE-derived metallic band develops upon the alkali encapsulation. Not only the s but the d orbital states of the Cs atom take part in the hybridization with the NFE state. Nevertheless, the resulting metallic band has almost the same energy dispersion as the intact NFE state. Using the first-principles electron dynamic simulations under applied electric fields, we calculated the field emission current of the BNNT and CNT. We found that the Cs-doped BNNT gives 2 orders of magnitude larger emission current than the CNT. We suggest that, combined with its intrinsic robustness against oxidation, the alkali metal-doped BNNT could be a highly efficient and stable electron field emitter.

Acknowledgment. This work has been supported by the A3 Foresight Program of KOSEF-NSFC-JSPS, the Ministry of Science and Technology of China (Grant No. 2006CB605105), and the National Natural Science Foundation of China (Grant No.10674077). N.P. appreciates the support from TND national project. C.P. and J.I. are supported by the SRC Program (Center for Nanotubes and Nanostructured Composites) of MOST/KOSEF.

Supporting Information Available: . Computational details for the field emission current of the Cs-doped (5,5) BNNT under the applied field of 0.2V/Å and electronic structures of pure and Cs-doped double-walled BNNT (DW-BNNT) and bundled DW-BNNT, BN nanoribbon, etc. This material is available free of charge via the Internet at http://pubs.acs.org.

JA805557G

(18) Shan, B.; Cho, K. *Phys. Rev. Lett.* **2005**, *94*, 236602.

(19) Terrones, M.; Charlier, J.-C.; Gloter, A.; Cruz-Silva, E.; Terrés, E.; Li, Y. B.; Vinu, A.; Zanolli, Z.; Dominguez, J. M.; Terrones, H.; Bando, Y.; Golberg, D. *Nano Lett.* **2008**, *8*, 1026.